

Modeling and simulation of ANN Linear Active Disturbance Rejection Control of D-STATCOM on Total Disturbance Error Compensation

Gaali Venkatajayadeep¹. Dr.P.Sujatha²

¹PG-Scholar, Department of EEE (Electrical Power Systems), JNTUA College of Engineering, Ananthapuramu, A.P., India.

² Professor, Department of EEE, JNTUA College of Engineering, Ananthapuramu., A.P., India.

Abstract: This study introduces a novel method to improve the performance of D-STATCOM by incorporating Linear Active Disturbance Rejection Control (LADRC). This controller forms the foundation of the proposed approach..The suggested controller is made to efficiently make up for the error brought on by the overall disturbance.Upon conducting a study, it has been determined that the enhanced Linear Active Disturbance Rejection Control (LADRC) has superior anti-interference capabilities when compared to conventional LADRC. The ANN (Artificial Neural Network) LADRC is employed as a substitute for the conventional D-STATCOM control method in the context of current inner loop control. This substitution yields enhanced control performance, tracking performance, and anti-interference performance in comparison to the proportional integral (PI) controller. The simulation findings demonstrate that the enhanced Linear Active Disturbance Rejection Control (LADRC) demonstrates enhanced performance over the Proportional

Integral (PI) controller. The results show that the ANN-LADRC controller surpasses the traditional PI controller in tracking accuracy and disturbance rejection capabilities.

Index terms: Static synchronous compensator in distribution, anti-disturbance, ANN control, and Linear Active Disturbance Rejection Control.

1.Introduction:

The implementation of D-STATCOM in power distribution networks offers a viable solution for mitigating voltage quality issues, including voltage fluctuation and flicker, voltage sags, and voltage unbalance [1-5] This technology exhibits a wide range of potential applications in power distribution networks, as well as in future networks incorporating micro-grids. The extent to which D-STATCOM can mitigate the issues is primarily contingent upon the efficacy of the controller for STATCOM. To improve the D-STATCOM's performance controller, researchers from both domestic and international backgrounds have made continuous endeavors in developing control

methods for the D-STATCOM. As a result, a range of control strategies have been provided by the researchers [6-12]. These control systems can be broadly categorized into three distinct groups. There are three main approaches to control systems. The first approach is the conventional Proportional-Integral-Derivative (PID) control. The second approach utilizes current control methods based on state space representation, including optimal tracking control and variable structure control.

The third approach is intelligent control, which encompasses methods like Artificial neural network control. Nevertheless, the conventional Proportional-Integral (PI) control method is primarily applicable to linear control systems. In the case of the D-STATCOM system, which exhibits nonlinear characteristics and the performance of the PI controller is unsatisfactory. Furthermore, The controller faces increased challenges in meeting its performance objectives when there are changes in the system's equivalent parameters or when uncertain external disturbances occur. The modern control theory, which relies on state equations, necessitates a precise mathematical model for optimal performance. However, achieving satisfactory control outcomes for complex

systems like the D STATCOM, which lack accurate mathematical models, is a challenge for modern control theory. When it comes to intelligent control, meeting the real-time control requirement poses a significant challenge. Furthermore, it is worth noting that voltage imbalance is not included in most of the control schemes stated above. Voltage imbalances are common in low-voltage distribution networks, making it crucial to choose an effective control strategy for D-STATCOM to maintain voltage magnitude and balance in line with established standards during uneven voltage conditions. The Active Disturbance Rejection Controller (ADRC) has proven effective in various power electronic applications, including PWM rectifiers, active power filters, and matrix converters,[13-15]). Due to its excellent dynamic performance, adaptability, and robustness. This paper examines the D-STATCOM system's characteristics and explores the limitations of PI control, modern control, and intelligent control. To overcome these shortcomings, this paper suggests using Active Disturbance Rejection Control (ADRC) for the D-STATCOM voltage controller. Furthermore, it employs a controller design that integrates positive-negative sequence voltage control loops. This method guarantees that both the magnitude

and the degree of imbalance of the Point of Common Coupling (PCC) voltage meet the standards for power supply voltage.

2.Design of D-STATCOM:

The D-STATCOM's operating mechanism is dependent on the control scheme that manages the energy transfer between the converter and the distribution grid. This control scheme is also impacted by the converter's secondary output voltage. This is how the basic operating concept might be summed up: If the D-STATCOM output voltage amplitude is greater than the network voltage, the D-STATCOM will inject reactive power when the current passes through the reactance and into the network. When the output voltage range of the converter is lower than that of the network, the D-STATCOM absorbs reactive power from the network, particularly when current flows towards the network. In contrast, when the converter's output voltage range matches that of the network, there's no exchange of reactive power, indicating a balanced state for the D-STATCOM. Equations (1) and (2) define the active and reactive powers injected by the D-STATCOM, respectively.

$$P_{ST} = \frac{V_{PCC}V_{ST}\sin\delta}{X_{ST}} \text{ --- (1)}$$

$$Q_{ST} = \frac{V_{PCC}(V_{PCC}-V_{ST}\cos\delta)}{X_{ST}} \text{ --- (2)}$$

The reactance of the coupling transformer is

denoted as X_{st} , and δ represents the phase shift angle between the voltages V_{pcc} and V_{st} . When the D-STATCOM operates continuously, it generates a voltage V_2 that is synchronized with V_{pcc} (with $\delta=0$), resulting in only reactive power flow ($P_{st}=0$). Reactive power is described by equation 2 as follows:

$$Q_{ST} = \frac{V_{PCC}(V_{PCC} - V_{ST})}{X_{ST}} \text{ --- (3)}$$

During continuous operation, the voltage V_{ST} is shifted laterally to stabilize the voltage V_{pcc} at the constant bus and to compensate for losses in the coupling transformer and the D-STATCOM switches, as shown in Figure 1. In this setup, the resistance symbolizes the active losses in the switches and transformer, which are counteracted by the series inductance

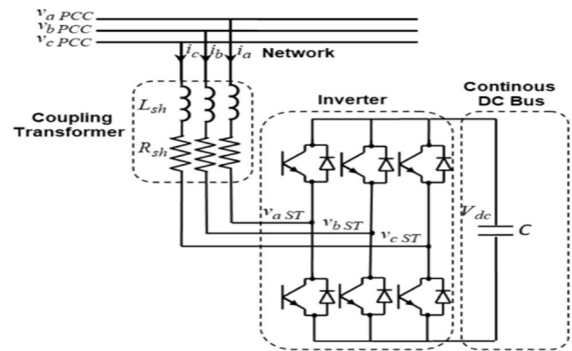


Fig1:Simplified Equivalent Diagram Of D-STATCOM

The performance of the grid-connected inverter significantly affects the power quality delivered by the D-STATCOM. There are two types of D-STATCOM systems: voltage source and current source,

differentiated by their input setups. The current source configuration necessitates a substantial series inductor on the DC side to ensure the stability of the DC current.

which can result in slower response times for the system. Consequently, grid-connected voltage source inverters are commonly preferred in industrial applications.

3. D-STATCOM Using LADRC:

The D-STATCOM control system is designed to regulate voltage and current within power systems through a double closed-loop structure. This structure comprises two feedback loops that collaboratively manage the system's performance. In this configuration, the outer voltage loop is responsible for generating the reference voltage, whereas the inner current loop creates the reference currents required by the system. Specifically, the outer loop generates reference currents for the d-axis and q-axis, known as i_{d-ref} and i_{q-ref} , respectively. These reference currents are then fed into the inner loop's feedback controller. The controller compares these reference currents with the actual currents and adjusts the system to ensure optimal operation. This dual-loop structure significantly enhances the D-STATCOM system's ability to maintain precise control

over voltage and current levels. Linear Active Disturbance Rejection Control (LADRC) is an advanced method utilized to counteract disturbances and stabilize system dynamics. It is particularly effective in controlling D-STATCOM systems.

In this setup, the q-axis current reference, i_{q-ref} , is usually obtained from the AC system bus voltage or through a reactive power control mechanism in the outer loop. On the other hand, the d-axis current reference, i_{d-ref} , is determined by the difference between the target capacitor voltage and the actual voltage observed.

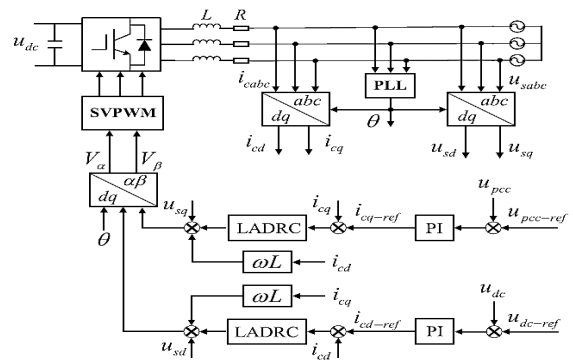


Fig 2. Control structure of D-STATCOM with LADRC

The mathematical representation of the D-STATCOM within a stationary three-phase coordinate system is described as follows:

$$L \frac{d}{dt} \begin{bmatrix} i_{ca} \\ i_{cb} \\ i_{cc} \end{bmatrix} = \begin{bmatrix} u_{sa} \\ u_{sb} \\ u_{sc} \end{bmatrix} - R \begin{bmatrix} i_{ca} \\ i_{cb} \\ i_{cc} \end{bmatrix} - \begin{bmatrix} u_{ca} \\ u_{cb} \\ u_{cc} \end{bmatrix} \dots \dots (4)$$

The DC side model is given as

$$C \frac{du_{dc}}{dt} = s_a i_{ca} + s_b i_{cb} + s_c i_{cc} - \frac{u_{dc}}{R_{dc}} \dots (5)$$

Among them the variability of the three-phase current over time complicates the design of the controller. Consequently, the mathematical model in the three-phase static coordinate system is converted into a two-phase synchronous rotating coordinate system by applying a coordinate transformation technique.. The transformation involves the following matrix:

$$P = \frac{2}{3} \begin{bmatrix} \cos\theta & \cos(\theta - \frac{2\pi}{3}) & \cos(\theta + \frac{2\pi}{3}) \\ -\sin\theta & -\sin(\theta - \frac{2\pi}{3}) & -\sin(\theta + \frac{2\pi}{3}) \\ \frac{\sqrt{2}}{2} & \frac{\sqrt{2}}{2} & \frac{\sqrt{2}}{2} \end{bmatrix} \dots (6)$$

The D-STATCOM is represented in the dq0 framework. The mathematical model is set within a rotating coordinate system [16].

$$L \frac{di_d}{dt} = \omega L i_q - R i_d - u_{s_d} - u_{L_d} \dots (7)$$

$$L \frac{di_q}{dt} = -\omega L i_d - R i_q - u_{s_q} - u_{L_q} \dots (8)$$

$$C \frac{du_{dc}}{dt} = \sqrt{\frac{3}{2}} (\cos\delta i_d + \sin\delta i_q) \dots (9)$$

Equations (8) and (9) explain that after the coordinate transformation, the grid side values on the d- and q-axes are denoted by

variables u_{sd} and u_{sq} , respectively. The voltage components of the D-STATCOM output voltage are represented by U_{ld} and U_{lq} . By analyzing the difference (δ) between the grid voltage and the D-STATCOM's output voltage, one can ascertain if the system is absorbing or generating reactive power. The D-STATCOM's voltage is synchronized with the external voltage, and the d-q components of both voltage and current are obtained from the output of the Phase Locked Loop (PLL). The i_{cq} current component is responsible for regulating reactive power, while the i_{cd} current component handles the regulation of active power. Based on these dynamics, this study develops a double closed-loop controller for the D-STATCOM system utilizing the Linearized Adaptive Dynamic Range Controller (LADRC). Within this framework, a LADRC-based controller operates the current inner loop, and a PI-based controller manages the voltage outer loop. The complete d-q vector control for the D-STATCOM system is depicted in Fig. 2. and Total Disturbance Compensation [17,18]. Fig4 depicts the control block diagram. When it comes down to it, anti-disturbance and stability are at the heart of the control system's main issue. Traditional control is provided using frequency domain analysis in reference [19]. The uncertainty of

the model parameter and the control input gain are both

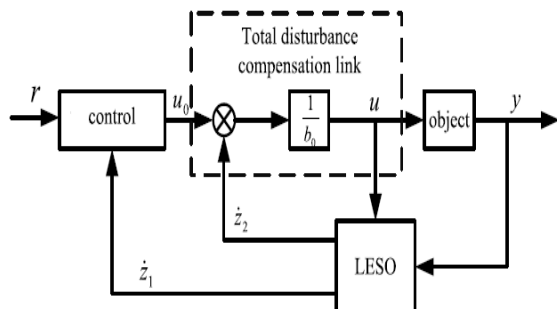


Fig 3: LADRC control block diagram.

taken into account in this LADRC study. The current tracking control link, employing a stability analysis technique, governs the three-phase, four-wire shunt active power filter (SAPF) of the converter. The PI controller manages both tracking and disturbance rejection within the evaluation system, whereas LADRC successfully resolves the conflict between tracking performance and disturbance rejection.

4. Artificial Neural Network (ANN):

In this part we'll go structure and education of Artificial Neural Network (ANN). Is a generalization of all The supervised learning-capable neural network paradigms . When artificial neural network (ANN) with knowledge dispersed over connection strengths, Studies and implementations of the ANN strategy have demonstrated the usefulness of combining

the strengths of neural network systems, particularly in areas like the direct adaptation of knowledge articulated as a set of ANN and the generalizability of existing algorithms.

network's overall input-output behavior is dictated by the values of a collection of movable parameters connected through its nodes. In this iteration, the gradient descent algorithm makes changes to the premise parameters in the direction of the past. The neural network's learning or training phase entails finding appropriate parameter values to ensure a good match with the training data. The error rate of ANN training can be decreased by employing different algorithms. For a more efficient search for the best parameters, we combine the gradient descent approach with a least squares algorithm. Since the search space dimensions of the backpropagation method employed in neural networks are decreased, the convergence of such a hybrid approach is significantly accelerated. To aid in the learning and adjusting processes, ANN employ the model embedded in an adaptive system architecture.

4.1 Architecture of ANN: The architecture of an ANN refers to its overall structure, including the arrangement of neurons, layers, and connections between them. Three layers are typically seen in an ANN. The input layer

is the uppermost layer, where input neurons are found. These neurons send data to the hidden layer beneath. After the hidden layer processes this data, it forwards the results to the output layer. This system includes elements such as a cost function, weights, and an activation function. The numerical values that represent the weight of the connection between neurons. The learning ability of a neural network is defined by the weights connecting its neurons. These connections are known as neuron weights. Each link in an artificial neural network determines its strength and is assigned a weight during the learning process. Each neuron normally has an associated bias, and these weights are modified during the training phase to maximize the network's performance which, as a constant term, enables the neuron to modify its output without regard to inputs. To provide non-linearity, each neuron in the network usually applies an activation function to the weighted sum of its inputs. In order to reduce the error between the expected and actual outputs, the backpropagation technique is employed during training to modify the weights of the connections in the network. In this process, the gradients of the loss function relative to the weights are calculated, and then optimization algorithms

like gradient descent are employed to appropriately adjust the weights.

Training process consists of inputting data into the network, comparing the network's predicted output to the actual output, and adjusting the weights within the network to reduce the error.

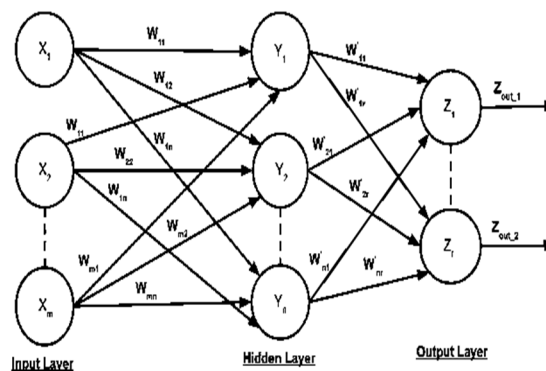


Fig 4 : Architecture of ANN

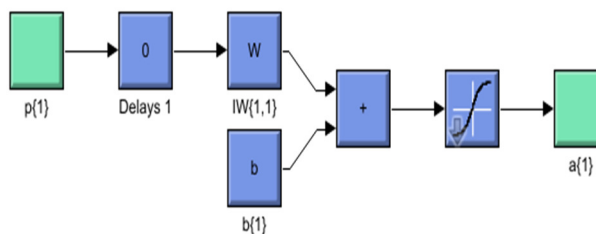
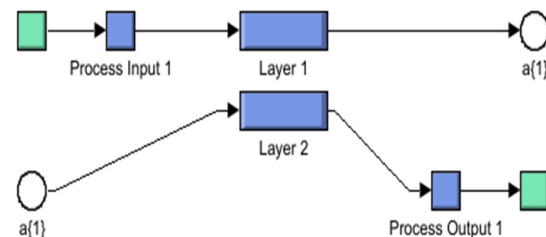


Fig 5 : Training process for ANN controller

5. ANN-LADRC:

In this study, the parameter adaptive controller utilizing ANN-LADRC adjusts the parameters of the LADRC controller based on the error (e), the rate of change of the error (\dot{e}), and the ANN-determined relationships between parameters. This method offers effective control and simplifies the adjustment of parameters. Known as ANN control, this application of ANN theory in control engineering emulates human learning and adaptability to environments. The ANN control system consists of three layers: the Input Layer, the Hidden Layer, and the Output Layer.

ANN control is useful for addressing a wide range of ambiguous issues since its not require a precise mathematical description of the controlled item. However, the system's control performance and dynamic quality are both diminished by the ANN processing of system input. Additionally, the ANN control's resistance to disturbance breaks down under heavy disturbance.

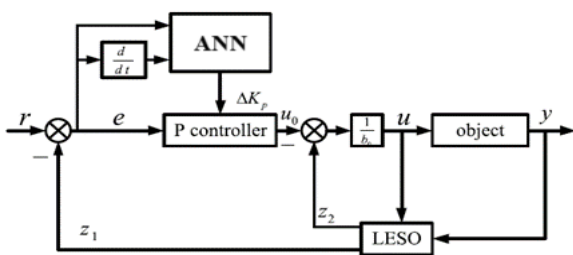


Fig6: ANN-LADRC block diagram

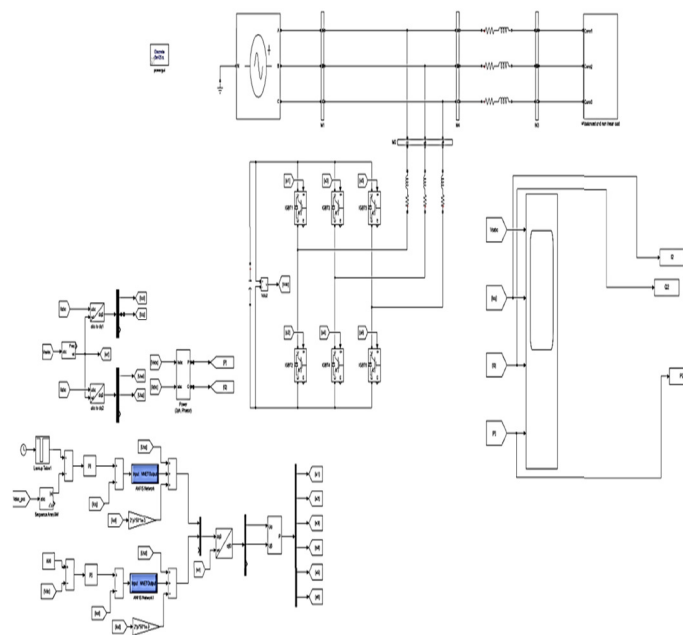


Fig 7 : Simulation digram of ANN-LADRC.

As seen in fig. 7, ANN is used in the simulation's design. In order to monitor source voltage and current, the three-phase, 380 V input voltage is coupled to the thphase series RLC branch between linked voltage and current measuring blocks. The IGBT inverter receives pulses from an ANN controller. The inverter and AC system are connected in parallel via a filter as the fundamental idea behind D-STATCOMBy correctly changing the switches of the power electronic devices in the inverter, reactive power compensation can be achieved by varying the amplitude and phase of the D-STATCOM input grid current.

TABLE: System parameters.

Symbol	Quantity	Value	unit
Q_b	Rated capacity	K_{var}	20
V_g	Base Voltage	v	380
f	Base frequency	Hz	50
U_{dc}	Dc-side bus voltage	v	800
C	Dc-side bus capacitor	μ	3000
L	Filter output inductance	mH	1
R	Filter output impedance	Ω	0.5

6.Results:

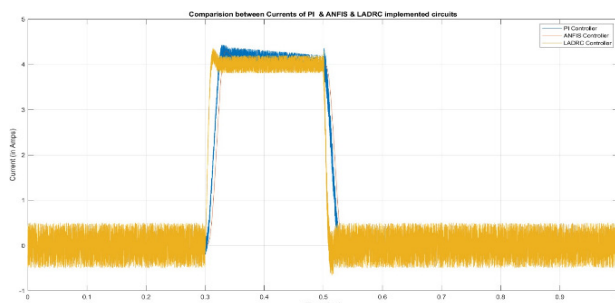


Fig 8: Comparison between Current of PI & LADRC & ANN implemented Controllers Under low voltage ride through.

Figure 8 illustrates that the current output from the D-STATCOM undergoes considerable fluctuations, leading to an extended period before reaching a stable state. This indicates that the PI controller is more susceptible to disturbances from grid-side faults. Unlike the PI controller, the

LADRC shows reduced sensitivity to grid-side disturbances. Its performance is less affected by voltage faults, leading to more stable current output with quicker response times. Implementing an ANN controller further improves performance by minimizing fluctuations and enhancing resilience against grid voltage faults. Its superior anti-interference capabilities contribute to smoother operation and faster stabilization compared to both the PI and LADRC controllers.

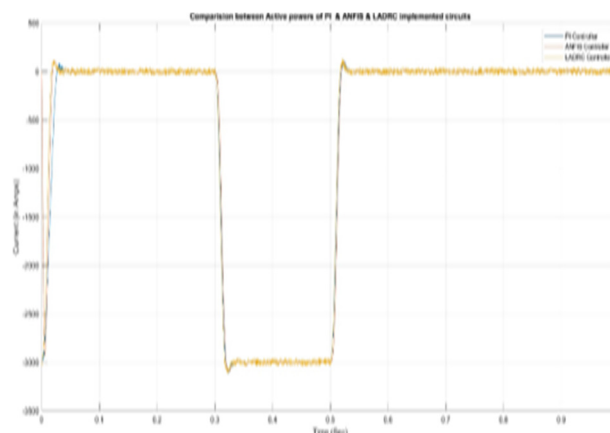


Fig 9: Comparison between active power of PI & LADRC & ANN implemented Controllers Under low voltage ride through.

Fig 9 shows the When employing a PI controller, the D-STATCOM's active power output exhibits significant fluctuations during symmetrical grid faults. This leads to prolonged stabilization time, affecting the accuracy of power tracking. Implementation of LADRC shows reduced susceptibility to

grid-side disturbances compared to the PI controller. Consequently, the D-STATCOM achieves quicker stabilization and maintains better active power tracking accuracy under symmetrical faults. Utilizing an ANN controller further mitigates fluctuations in active power output and enhances resilience against grid voltage faults. Its superior anti-interference capabilities ensure smoother operation and more accurate power tracking, even in challenging grid conditions.

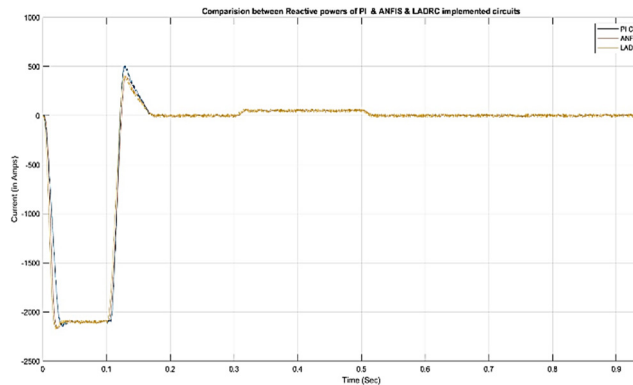


Fig 10: Comparison between Reactive power of PI & LADRC & ANN implemented Controllers Under low voltage ride through.

Fig 10 shows the When employing a PI controller, the D-STATCOM's reactive power output exhibits significant fluctuations during symmetrical grid faults. This leads to prolonged stabilization time, affecting the accuracy of power tracking. Implementation of LADRC shows reduced susceptibility to grid-side disturbances compared to the PI controller. Consequently, the D-STATCOM

achieves quicker stabilization and maintains better reactive power tracking accuracy under symmetrical faults. Utilizing an ANN controller further mitigates fluctuations in active power output and enhances resilience against grid voltage faults. Its superior anti-interference capabilities ensure smoother operation and more accurate power tracking, even in challenging grid conditions.

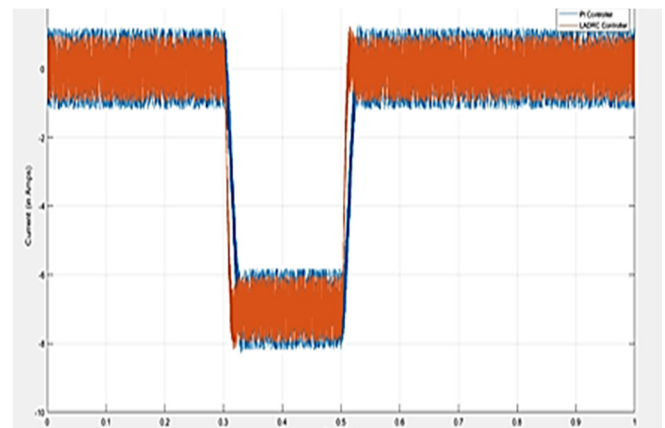


Fig 11: Comparison between Current of PI & LADRC implemented Controllers Under Increasing and decreasing load.

Fig 11 shows the When operated under a PI controller, the D-STATCOM exhibits relatively slower adjustment times and longer periods to reach a steady state. Additionally, the output current fluctuates greatly, impacting the stability of the system. Implementing LADRC results in significantly faster adjustments and improved tracking performance of the D-STATCOM. The system demonstrates quick adaptation to load changes, leading to stable operation in a shorter time frame. Moreover, the output current remains more consistent,

indicating the robust anti-interference capabilities of LADRC.

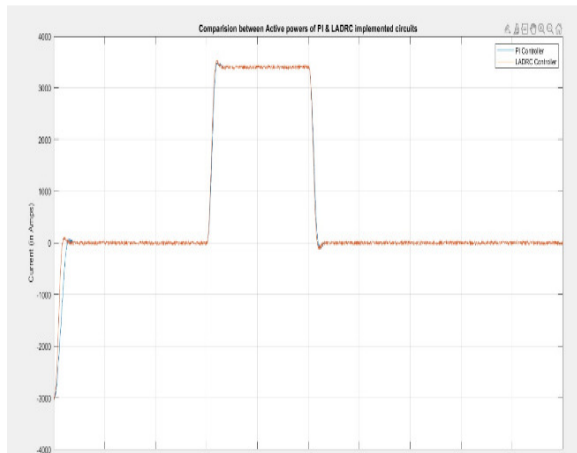


Fig 12: Comparison between Current of PI & LADRC implemented Controllers Under Increasing and decreasing load.

Fig 12 shows the Under the operation of a PI controller, the D-STATCOM experiences relatively prolonged adjustment times and requires a longer duration to stabilize. Additionally, the output power fluctuates significantly, impacting the system's stability. By employing LADRC, the D-STATCOM demonstrates fast adjustments and excellent tracking performance. It swiftly adapts to grid load changes, reaching a steady state in a shorter timeframe. Moreover, the output power remains stable, indicating the robust anti-interference capabilities of LADRC.

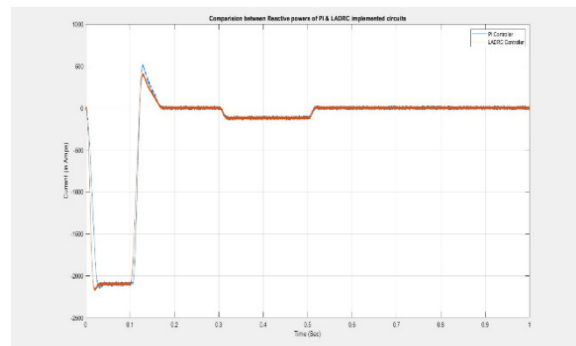


Fig 13: Comparison between Reactive power of PI & LADRC implemented Controllers Under Increasing and decreasing load

Fig 13 shows that When controlled by a PI controller, the D-STATCOM exhibits relatively slow adjustment times and requires a longer duration to stabilize. Moreover, the output reactive power fluctuates significantly, affecting system stability.

Implementing LADRC results in rapid adjustments and excellent tracking performance of the D-STATCOM. It swiftly responds to grid load changes, reaching a steady state more quickly. Additionally, the output reactive power remains stable, showcasing the robust anti-interference abilities of LADRC.

To verify the effectiveness of the new system, its reactive current tracking performance is tested using a three-phase symmetrical fault in grid voltage and load variations as an example.

(I) The voltage at the grid connection point symmetrically drops to 0.5 p.u. at $t = 0.3s$ and

returns to normal at $t = 0.5s$. (II) At $t = 0.3s$, the load is increased by 100%, and then at t it returns to the initial setting.

Under PI control, the D-STATCOM's reactive current output swings considerably and takes a while to stabilize when the three-phase voltage falls to 50%. It demonstrates how the grid side voltage drop has a significant impact on the PI controller and how poor its anti-interference capability is. The outcomes demonstrate the superiority of the ANN-LADRC controller over the conventional PI controller in terms of tracking and anti-disturbance skills. The PI controller's tracking and anti-disturbance capabilities are inversely correlated with the evaluation system's anti-disturbance capabilities, and LADRC effectively resolves this contradiction. The findings demonstrate that the ANN-LADRC controller outperforms the conventional PI controller in terms of disturbance rejection and tracking. The ANN-LADRC can successfully estimate and correct for large-scale system disturbances, resolving the conflict between "tracking" and "disturbance resistance" that plagues typical PI controllers.

7. THD (Total Harmonic Distortion): In non-linear loads, Total Harmonic Distortion (THD) refers to the distortion in the current waveform caused by the non-linear behavior

of the load. Non-linear loads are those that draw a non-sinusoidal current waveform from the power supply, such as electronic devices with rectifiers or switching power supplies. These loads introduce harmonics into the electrical system, resulting in increased THD levels. High THD in non-linear loads can lead to various issues including overheating of transformers, increased losses in electrical equipment, and interference with sensitive electronic equipment. Managing THD in nonlinear loads is essential for maintaining power quality and ensuring the reliable operation of electrical systems. The Total Harmonic Distortion (THD) of the Artificial Neural Network (ANN) Linear Active Disturbance Rejection Control (LADRC) of a D-STATCOM (Distribution Static Synchronous Compensator) on Total Disturbance Error Compensation refers to the amount of harmonic distortion present in the compensation signal generated by this control system to mitigate disturbances in a power system. In simpler terms, this means evaluating how effectively the ANN-LADRC control algorithm implemented in a D-STATCOM can compensate for disturbances in a power system while minimizing the distortion it introduces to the system's waveform. THD analysis in this

context helps assess the performance and efficiency of the control strategy in terms of both disturbance rejection and harmonic mitigation

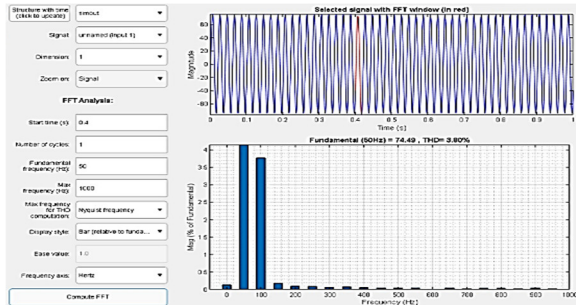


Fig13: THD with PI controller of current is 3.38

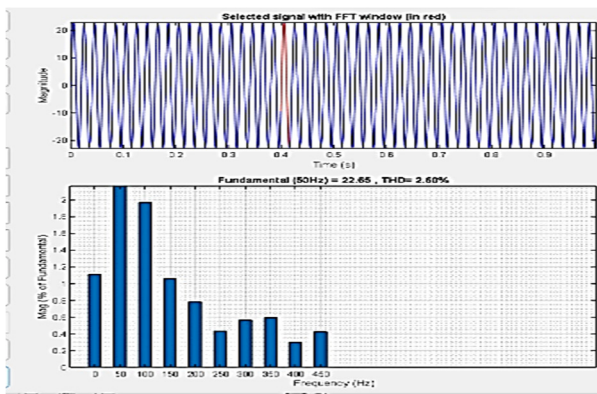


Fig14:: THD with LADRC controller of current is 2.60

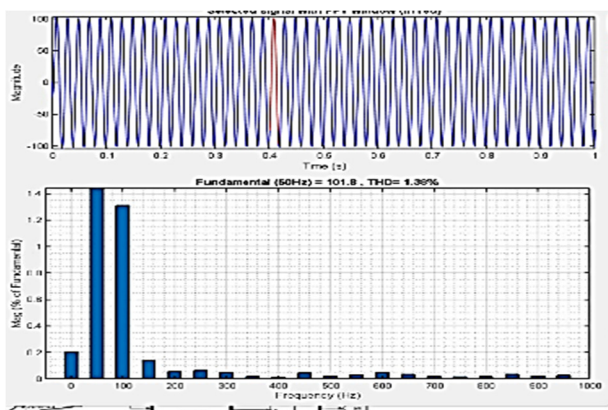


Fig 15 : THD with ANN controller of current is 1.38.

comparing Total Harmonic Distortion (THD) of current for different types of controllers. THD values indicate the level of distortion in the current waveform. In your comparison:

PI controller has a THD of 3.38.

LADRC controller has a THD of 2.60.

ANN controller has a THD of 1.38.

Lower THD values generally indicate better performance in terms of current waveform quality, as they represent less distortion. Therefore, the ANN controller seems to provide the cleanest current waveform

9. Conclusion:

This research introduces an Disturbance Rejection Control (LADRC) method for the internal current loop of the D-STATCOM system, considering its nonlinear, multivariable, and strongly coupled characteristics.

This study presents a novel contribution in the form of a Linear Active Disturbance Rejection Controller, which aims to enhance the control performance of the overall control system by effectively compensating for the total disturbance error. The user's text is too brief to be rewritten academically. The findings indicate that the ANN-LADRC controller exhibits superior disturbance rejection and tracking performance compared to the conventional PI controller. The ANN-LADRC demonstrates effective estimation

and compensation of disturbances, particularly in scenarios where significant disruptions occur inside the system. This capability addresses the inherent conflict between "tracking" and "disturbance resistance" encountered with conventional PI controllers. Based on the comparison, it appears that using the ANN controller leads to significantly lower Total Harmonic Distortion (THD) compared to PI and LADRC controller. Therefore, in the context of minimizing distortion and improving the quality of the output waveform, the ANN controller demonstrates superior performance.

References:

- [1] H. Bakir and A. A. Kulaksiz, "Modelling and voltage control of the solarwind hybrid micro-grid with optimized STATCOM using GA and BFA," *Eng. Sci. Technol., Int. J.*, vol. 23, no. 3, pp. 576–584, Jun. 2020.
- [2] S. R. Marjani, V. Talavat, and S. Galvani, "Optimal allocation of DSTATCOM and reconfiguration in radial distribution network using MOPSO algorithm in TOPSIS framework," *Int. Trans. Electr. Energy Syst.*, vol. 29, no. 2, p. e 2723, 2019.
- [3] S. Rezaeian-Marjani, S. Galvani, V. Talavat, and M. Farhadi-Kangarlu, "Optimal allocation of D-STATCOM in distribution networks including correlated renewable energy sources," *Int. J. Electr. Power Energy Syst.*, vol. 122, Nov. 2020, Art. no. 106178.
- [4] R. O. de Sousa, A. F. Cupertino, L. M. F. Morais, and H. A. Pereira, "Minimum voltage control for reliability improvement in modular multilevel cascade converters based STATCOM," *Microelectron. Rel.*, vol. 110, Jul. 2020, Art. no. 113693.
- [5] W. Xiao, J. Li, and Y. Wang, "Study on reactive power compensation strategy based on STATCOM," *Power Capacitor Reactive Power Compensation*, vol. 40, no. 6, pp. 24–29, 2019.
- [6] S. N. Duarte, B. C. Souza, P. M. Almeida, L. R. Araujo, and P. G. Barbosa, "Control algorithm for DSTATCOM to compensate consumer-generated negative and zero sequence voltage unbalance," *Int. J. Electr. Power Energy Syst.*, vol. 120, Sep. 2020, Art. no. 105957.
- [7] A. Ghias, P. Jose, and V. G. Agelidis, "A novel control method for transformerless H-bridge cascaded STATCOM with star configuration," *IEEE Trans. Power Electron.*, vol. 30, no. 3, pp. 1189–1202, Mar. 2015.

- [8] P. Wang, Y. Wang, N. Jiang, and W. Gu, "A comprehensive improved coordinated control strategy for a STATCOM integrated HVDC system with enhanced steady/transient state behaviors," *Int. J. Electr. Power Energy Syst.*, vol. 121, Oct. 2020, Art. no. 106091.
- [9] J. Wang and W. Wang, "Self-tuning of PID parameters based on particle swarm optimization," *Control Decis.*, no. 1, pp. 73–76 and 81, 2005.
- [10] J. Tang, A. Luo, and K. Zhou, "Variable structure neural network Neural Network control for STATCOM," *J. Hunan Univ., Natural Sci.*, no. 7, pp. 48–52, 2007.
- [11] D. Amoozegar, "DSTATCOM modelling for voltage stability with Neural Network logic PI current controller," *Int. J. Electr. Power Energy Syst.*, vol. 76, pp. 129–135, Mar. 2016.
- [12] K. D. E. Kerrouche, E. Lodhi, M. B. Kerrouche, L. Wang, F. Zhu, and G. Xiong, "Modeling and design of the improved D-STATCOM control for power distribution grid," *Social Netw. Appl. Sci.*, vol. 2, no. 9, pp. 1–11, Sep. 2020.
- [13] A. Halder, N. Pal, and D. Mondal, "Higher order sliding mode STATCOM control for power system stability improvement," *Math. Comput. Simul.*, vol. 177, pp. 244–262, Nov. 2020.
- [14] S. Li, L. Xu, and T. A. Haskew, "Control of VSC-based STATCOM using conventional and direct-current vector control strategies," *Int. J. Electr. Power Energy Syst.*, vol. 45, no. 1, pp. 175–186, Feb. 2013.
- [15] M. R. Tavana, M.-H. Khooban, and T. Niknam, "Adaptive PI controller to voltage regulation in power systems: STATCOM as a case study," *ISA Trans.*, vol. 66, pp. 325–334, Jan. 2017.
- [16] S. Vachirasricirikul, I. Ngamroo, and S. Kaitwanidvilai, "Coordinated SVC and AVR for robust voltage control in a hybrid wind-diesel system," *Energy Convers. Manage.*, vol. 51, no. 12, pp. 2383–2393, 2010.
- [17] J. Han, "Auto-disturbances-rejection controller and its applications," *Control Decis.*, no. 1, pp. 19–23, 1998.
- [18] Q. Zheng, L. Dong, D. H. Lee, and Z. Gao, "Active disturbance rejection control for MEMS gyroscopes," *IEEE Trans. Control Syst. Technol.*, vol. 17, no. 6, pp. 1432–1438, Nov. 2009.